IEEE Access
Multidisciplinary : Rapid Review : Open Access Journal

Received 30 September 2022, accepted 28 October 2022, date of publication 1 November 2022, date of current version 4 November 2022.

*Digital Object Identifier 10.1109/ACCESS.2022.3218633*

RESEARCH ARTICLE

# Blind Separation for Wireless Communication Convolutive Mixtures Based on Denoising IVA

**MINGCHUN LI[1], ZHENGWEI CHANG[2], LINGHAO ZHANG[2], HOUDONG XU[3], ZHONGQIANG LUO[1,4], (Member, IEEE), AND RUIMING GUO[1]**

[1]School of Automation and Information Engineering, Sichuan University of Science and Engineering, Yibin 644000, China
[2]State Grid Sichuan Electric Power Research Institute, Chengdu 610095, China
[3]State Grid Sichuan Electric Power Company, Chengdu 610095, China
[4]Artificial Intelligence Key Laboratory of Sichuan Province, Sichuan University of Science and Engineering, Yibin 644000, China

Corresponding author: Zhongqiang Luo (zhongqiangluo@gmail.com)

This work was supported in part by the National Natural Science Foundation of China under Grant 61801319, in part by Sichuan Science and Technology Program under Grant 2020JDJQ0061, 2021YFG0099, 2020JDJQ0075, in part by the 2022 Graduate Innovation Fund of Sichuan University of Science and Engineering under Grant Y2021062.

**ABSTRACT** In wireless communication systems, signal transmission through a channel can not avoid the influence of noise. When it reaches the receiver, it is accompanied by time delay and attenuation. Therefore, the observed mixture signals at the receiver are convolutional mixed signals with noise contamination. To solve the problem of traditional frequency-domain based convolutive blind signal separation methods have poor separation performance for convolutional mixed signals with noise, this paper propose a denoise-FastIVA method to separate convolutional mixed signals with noise. The basic principle is to use a wavelet transform to denoise the observation signal, reduce the effect of noise on the separation effect of the algorithm, and enhance the robustness of the fast fixed-point independent vector analysis (FastIVA) separation algorithm to noise. Simulation experiments show the effectiveness of a denoise-FastIVA, under the condition that the baseband signal of binary phase shift keying (BPSK) and binary frequency shift keying (2FSK) signal modulation signal is 10 bits respectively,the separation accuracy of linear frequency modulization (LFM) has increased from 87% to more than 94%; BPSK has risen from 83% to over 97%; 2FSK has improved from 81% to over 95%. When the SNR is greater than 10 dB, the separation similarity of denoise-FastIVA for the communication mixed signals is more than 90%, and the demixing signal can demodulate the baseband signal completely and correctly. Baseband signals of experimental BPSK and 2FSK signal modulation signals are 100 bits respectively. When the signal-to-noise ratio is greater than 5dB, the signal separated by denoise-FastIVA method has the highest similarity coefficient with the source signal, and the bit error rate (BER) of the separated BPSK signal and the separated 2FSK signal are the lowest, compared with the traditional frequency domain demixing method and FastIVA algorithm.

**INDEX TERMS** Blind source separation, FastIVA, convolution mixing, IVA, wavelet denoising.

## I. INTRODUCTION

Blind source/signal separation (BSS) [1], [2] refers to the method of estimating the source signal only from the received signals. Independent component analysis (ICA) [3], [4] is a typical blind signal processing technique used to separate independent and non-Gaussian mixed signals with statistical properties, and is mainly suitable for the separation of linear instantaneous mixed observation signals. The instantaneous mixing model which only considers the direct path from transmitter to receiver is too ideal. In the actual wireless communication system, the communication signal arrives at the receiving antenna through different paths, with varying degrees of attenuation and delay. In the process of signal

The associate editor coordinating the review of this manuscript and approving it for publication was Easter Selvan Suviseshamuthu.

transmission, there must be noise effect. The observed signal received by the receiver is a convolutional mixed signal with noise.

At present, the most common denoising method used in wireless communication systems is wavelet denoising [5], [6]. Wavelet threshold denoising [6] is based on the corresponding different coefficients of signal and noise in the wavelet decomposition, and the wavelet coefficients between the two are negatively correlated. The effective signal is extracted by selecting an appropriate threshold value to achieve the purpose of noise removal. In the latest research, BSS is also used in signal denoising. For the Ground-based Synthetic Aperture Radar (GBSAR) technology to obtain noise in the dynamic deflection data of bridges, Xianglei Liu et al. proposed a single channel blind source separation signal (SCBSS) denoising method to obtain the dynamic deflection of the denoised bridge [7]. For noise in magnetotelluric (MT) sounding data, Rui Zhou et al. improving the traditional FastICA method, useful signal is well separated from noise. The correlation coefficient is used to calculate the number of field sources, and the fast iterative shrinkage threshold algorithm (FISTA) is used to adjust the decomposition of signal amplitude before and after FastICA [8].

The BSS of convolved mixture problem is mainly solved by the frequency domain method. This method uses the short-time Fourier transform (STFT) to convert the time domain convolutional mixing model to the instantaneous mixing model in the frequency domain, and then the ICA method is used for separation to obtain the frequency domain demixing signal. Finally the obtained frequency domain demixng signal is transformed back into the time domain to gain the time domain estimation of the source signal. This method is called frequency domain independent component analysis (FDICA) [9], [10], [11]. However, the problem with FDICA method is that the sorting of demixing signals is random and uncertain. To solve the separation problem of FDICA method, it is necessary to sort the separation signals of each frequency point. There are two main sorting methods at present. The first is to use the phase information between the spectrums to cluster the independent components at each frequency point using the estimated direction of arrival (DoA) [10] of the signal at each frequency point as a feature to solve the random uncertainty of sorting the separated signal. The second method is to use the amplitude information of the signal spectrum, and the signal correlation between adjacent frequency points of the same source signal is greater than that between adjacent frequency points of different source signal [11]. However, the robustness of this method is poor, resulting in unstable algorithm separation.

Another effective way to solve the uncertainty of FDICA random ordering is Independent Vector Analysis (IVA) [12], [13], [14], [15], [16], [17]. The IVA method is an extension of ICA and can solve the problem of BSS in frequency domain very well. The IVA method extends the univariate function in ICA to the multivariate function as the score function, which makes the data between different frequency points not separate but related. Thus, the problem of uncertain ordering of ICA method is solved by using this dependence between frequency points. The existing literature on IVA mainly focuses on voice signal [16] and image signal [17], and in most cases, the influence of noise is directly ignored. Noise is a non-negligible factor in the actual wireless communication system. In the literature [18], BPSK signals are separated from various kinds of interference blindly, but the anti-noise performance of the algorithm is not strong. The purpose of this paper is to propose a denoising IVA algorithm for blind convolutional mixing frequency domain separation in communication systems.

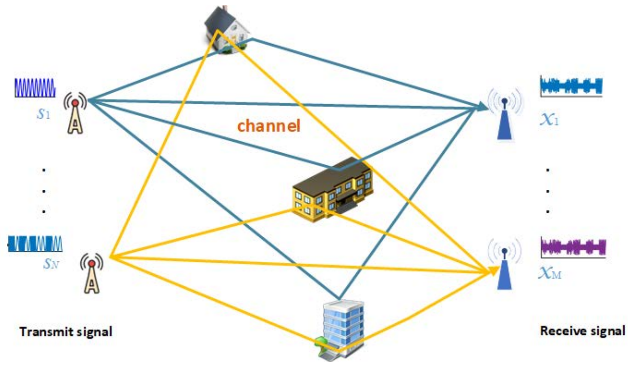

**FIGURE 1.** Convolution mixing model.

## II. PROBLEM DESCRIPTION

In the actual communication system, when the signal is transmitted through the wireless channel, noise is an important factor that can not be ignored, and there will be varying degrees of attenuation and delay when the signal reaches the receiver. In other words, the signal observed by the receiver is a convolutional mixed signal with noise.

Now suppose $N$ independent source signals $\mathbf{s}(t) = [s_1(t), s_2(t), \ldots, s_N(t)]^T$ are transmitted over a wireless channel and $M$ observation signals $\mathbf{x}(t) = [x_1(t), x_2(t), \cdots, x_M(t)]^T$ are received at the receiving end. Here we only consider additive white Gaussian noise. The simplified convolution mixing model is shown in Figure 1:

The specific mathematical expression is

$$\begin{aligned} x_i(t) &= \sum_{j=1}^{N} h_{ij}(t) * s_j(t) + n_i(t) \\ &= \sum_{j=1}^{N} \sum_{k=0}^{P-1} h_{ij}(k) s_j(t-k) + n_i(t), \; 1 \leq i \leq M \end{aligned} \tag{1}$$

where, $*$ is the convolution operator; $h_{ji}$ is the coefficients of an unknown mixed matrix $\mathbf{H}$; $P$ represents the length of the filter and $n_i(t)$ is the noise in the $ith$ observed signal.

The convolution model can be expressed in vector form

$$\mathbf{x} = \mathbf{H} * \mathbf{s} + \mathbf{n} \tag{2}$$

where, $*$ is the convolution operator; $\mathbf{x} \in \mathbb{C}^{M\times 1}$ is the observed signal; $\mathbf{H} \in \mathbb{C}^{M\times N}$ is mixed matrix; $\mathbf{s} \in \mathbb{C}^{N\times 1}$ is the source signal; $\mathbf{n} \in \mathbb{C}^{N\times 1}$ and is noise.

Time domain convolution mixed signal is transformed into frequency domain by STFT

$$\mathbf{x}_i(\omega) = \sum_{j=1}^{N} \mathbf{h}_{ij}(\omega)\mathbf{s}_j(\omega) + \mathbf{n}_i(\omega) 1 \le i \le M \tag{3}$$

where, $\mathbf{x}_i(\omega) = \left[x_i^1, x_i^2 \cdots, x_i^F\right]$ is the frequency domain signal of STFT of the $i$th observation signal; $\mathbf{s}_j(\omega) = \left[s_j^1, s_j^2 \cdots, s_j^F\right]$ is the frequency domain signal of STFT of the $j$th source signal. $\mathbf{h}_{ij}(\omega)$ and $\mathbf{n}_i(\omega)$ are the corresponding coefficient matrix and noise.

Frequency domain index does not affect the derivation of the algorithm, so it is ignored in the subsequent derivation. When the time-domain convolution mixed signal is transformed into the frequency domain by STFT, the following relationship exists at each frequency point

$$\mathbf{x}^f = \mathbf{H}^f \mathbf{s}^f + \mathbf{n}^f, \quad f = 1, \cdots, F. \tag{4}$$

where, $\mathbf{x}^f = \left[x_1^f, x_2^f, \cdots, x_M^f\right]$ and $\mathbf{s}^f = \left[s_1^f, s_2^f, \cdots, s_N^f\right]$ are the observed signal and source signal at frequency point $f$, respectively. $\mathbf{H}^f$ is the coefficient matrix of the frequency point $f$, and $\mathbf{n}^f$ is the noise of frequency point $f$.

In the derivation of IVA algorithm, it is assumed that the observed signal does not contain noise.The ideal observation signal is $\tilde{\mathbf{x}}$. The mixing model is $\tilde{\mathbf{x}} = \mathbf{H} * \mathbf{s}$ and the frequency domain model is $\tilde{\mathbf{x}}^f = \mathbf{H}^f \mathbf{s}^f$.Therefore, the estimated source signal can be obtained by finding a demixing matrix $\mathbf{w}^f$ at each frequency point. Estimated source signal without noise is $\tilde{\mathbf{s}}^f = \mathbf{w}^f \tilde{\mathbf{x}}^f = \mathbf{w}^f \mathbf{H}^f \mathbf{s}^f$.

If the actual noisy convolutional mixed signals are separated directly by the IVA method, the following relationships exist

$$\mathbf{y}^f = \mathbf{w}^f \mathbf{x}^f = \mathbf{w}^f \left(\tilde{\mathbf{x}}^f + \mathbf{n}^f\right) = \tilde{\mathbf{s}}^f + \mathbf{n}^f, f = 1, \cdots, F. \tag{5}$$

where, $\mathbf{y}^f = \left[y_1^f, y_2^f, \cdots, y_N^f\right]$ represents the actual demixing signal estimated at frequency point $f$.

The frequency domain estimation signal $\mathbf{y}_j = \left[y_i^1, \cdots, y_i^F\right]$, $i = 1, \cdots N$. is obtained by combining the signals of each frequency point, and then the frequency domain signal is transformed back to the time domain by inverse short-time Fourier transformation (ISTFT) to get the estimated source signal $\tilde{s}_j(t)$, $1 \le j \le N$.

## III. DENOISING INDEPENDENT VECTOR ANALYSIS ALGORITHM

Formula (5) shows that the observed signal with noise is separated directly, and separation results are affected by noise. In this case, a noise reduction independent vector analysis algorithm named deniose-FastIVA is presented. The algorithm flow is shown in Fig. 2,

Source signal $\mathbf{s}(t)$ passes through a noisy channel and receives observation signal $\mathbf{x}(t)$ at the receiver; $\mathbf{x}(t)$ is denoised by a wavelet threshold to get convolution mixed signal $\hat{\mathbf{x}}(t)$; then $\hat{\mathbf{x}}(t)$ is transformed STFT to get frequency domain mixed signal $\hat{\mathbf{x}}(\omega)$. Afterwards FastIVA algorithm is used to separate $\hat{\mathbf{x}}(\omega)$ to get the estimated source signal $\hat{\mathbf{y}}(\omega)$. Finally, $\hat{\mathbf{y}}(\omega)$ is transformed back to the time domain by ISTFT, resulting in the estimated source signal $\hat{\mathbf{s}}(t)$.

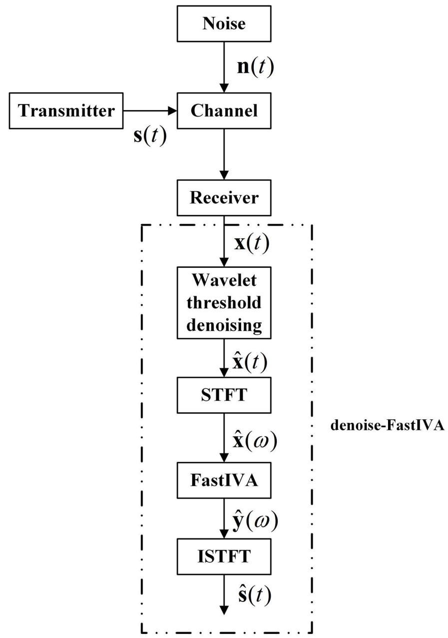


**FIGURE 2.** Flowchart of denoise-FastIVA algorithm.

### A. WAVELET THRESHOLD DENOISING

The wavelet threshold denoising method is based on the difference of the wavelet coefficients between the signal and the noise wavelet transform. To achieve the purpose of noise removal, an appropriate threshold function is used to gain an effective signal.

#### 1) WAVELET TRANSFORM

Obtain observation signal at receiver $\mathbf{x}(t)$, wavelet transform (WT) is applied to $\mathbf{x}(t)$, and the formula is as follows

$$WT_{x_i}(\alpha, \tau) = \frac{1}{\sqrt{\alpha}} \int_{-\infty}^{+\infty} x_i(t)\psi^*\left(\frac{t-\tau}{\alpha}\right) dt, \alpha > 0 \tag{6}$$

where, $WT_{x_i}(\alpha, \tau)$ is the coefficient of wavelet transform, $(\cdot)^*$ means the conjugation of the matrix, $\alpha$ represents the scale function, and $\tau$ is the distance of the shift.

In the process of actual engineering signal or time series processing, discrete wavelet transform (DWT) is often used to process engineering signal or time series. Discrete parameters in wavelet functions:

$$\left(W_\psi x_i\right)(\alpha, \tau) = \left\langle x_i(t), \psi_{\alpha,\tau}\right\rangle, i = 1, \cdots M. \tag{7}$$

Discretize the $\alpha$ and $\tau$ parameters in (7), $\alpha = 2^{-j}$, $\tau = 2^{-j}k$, $j, k \in Z$. Thus, discrete wavelet transform

$$\left(DW_\psi x_i\right)(j, k) = \left\langle x_i(n), \psi_{j,k}(n)\right\rangle$$
$$\psi_{j,k}(t) = 2^{\frac{j}{2}}\psi\left(2^j n - k\right), j, k \in Z. \tag{8}$$

In (6), $\psi(x)$ employs Haar wavelets, and the wave function is

$$\psi = \begin{cases} 1, & 0 \le x \le \frac{1}{2} \\ -1, & \frac{1}{2} \le x \le 1 \\ 0, & \text{others} . \end{cases} \tag{9}$$

where $x$ is a dummy variable.

### 2) THRESHOLD FUNCTION

$x_i(t)$ corresponding wavelet coefficient $DW_\psi x_i$ is obtained through DWT. Based on model $x_i(t) = \sum_{j=1}^{N} h_{ij}(t) * s_j(t) + n_i(t)$. Choose an appropriate threshold to get a useful signal, this article makes use of unbiased risk estimation thresholds (rigrsure). The absolute value of each element in signal $x_i$ whose length is L is sorted from small to large, then the elements are squared to get a new signal sequence.

$$f(k) = (\text{sort}(|x_k|))^2, (k = 0, 1, 2 \cdots L - 1) \tag{10}$$

If the threshold value is the square root of the $k$-th element of $f(k)$, that is $\lambda_k = \sqrt{f(k)}$. The risk from this threshold is

$$\mathbf{Risk}(k) = \left[ L - 2k + \sum^{k} f(j) + (L-k)f(L-k) \right] / L. \tag{11}$$

Threshold $\lambda = \sqrt{f(k_{\min})}$ is obtained from the value corresponding to the minimum value in $\mathbf{Risk}(k)$. The threshold function uses the soft threshold function, which is

$$\hat{\omega}_{j,k} = \begin{cases} \text{sgn}(\boldsymbol{\omega}_{j,k})(|\boldsymbol{\omega}_{j,k}| - \lambda), & |\omega_{j,k}| \ge \lambda \\ 0 & |\omega_{j,k}| < \lambda. \end{cases} \tag{12}$$

where, $\boldsymbol{\omega}_{j,k}$ is the wavelet coefficient vector and $\lambda$ is the picked threshold.

The denoised mixed signal $\hat{\mathbf{x}}(t)$ is gained from reconstructing the wavelet coefficients selected by the threshold.

## B. INDEPENDENT VECTOR ANALYSIS

After the observed signal passes through the wavelet threshold denoising method, the current mixed signal $\hat{\mathbf{x}}(t) = [\hat{x}_1(t), \hat{x}_2(t), \cdots, \hat{x}_M(t)]^T$ can be expressed as

$$\hat{\mathbf{x}} = \mathbf{H}^* \mathbf{s} \tag{13}$$

where, $*$ is the convolution operator, $\mathbf{H} \in \mathbb{C}^{M \times N}$ is an unknown mixed matrix, $\mathbf{s} \in \mathbb{C}^{N \times 1}$ is source signal.

Transform $\hat{\mathbf{x}}(t)$ to below frequency domain taking advantage of STFT method

$$\hat{\mathbf{x}}_i = \sum_{j=1}^{N} \mathbf{h}_{ij} \mathbf{s}_j \quad 1 \le i \le M. \tag{14}$$

where, $\hat{\mathbf{x}}_i = [\hat{x}_i^1, \hat{x}_i^2 \cdots, \hat{x}_i^F]$ represents the frequency domain signal of the $i$th mixed signal. The relation of each frequency point can be expressed as

$$\hat{\mathbf{x}}^f = \mathbf{H}^f \mathbf{s}^f \quad f = 1, \cdots, F. \tag{15}$$

By finding the demixing matrix $\mathbf{w}^f$ for each frequency point, the estimated source signal, $\hat{\mathbf{y}}^f$, can be obtained.

$$\hat{\mathbf{y}}^f = \mathbf{w}^f \hat{\mathbf{x}}^f \quad f = 1, \cdots, F. \tag{16}$$

where, $\hat{\mathbf{y}}^f = [\hat{y}_1^f, \hat{y}_2^f, \cdots, \hat{y}_N^f]$ is the demixing signal of the de-noised observed signal estimated at frequency point $f$. The $i$th source signal, $\hat{\mathbf{y}}_i = [\hat{y}_i^1, \hat{y}_i^2, \cdots, \hat{y}_i^F]$, is obtained by estimating the signal at each frequency point.

### 1) COST FUNCTION OF IVA

The cost function of the IVA algorithm is to separate the observed signals by maximizing the independence of the output signal $\hat{y}_i$. It can also be achieved by minimizing the mutual information between the estimated source component vectors.

The cost function of IVA algorithm is expressed by mutual information

$$I(\hat{\mathbf{y}}) = KL\left(p_{\hat{\mathbf{y}}} \| \prod_i p_{\hat{\mathbf{y}}_i}\right) = \int p_{\hat{\mathbf{y}}}(z) \log \frac{p_{\hat{\mathbf{y}}}(z)}{\prod_i p_{\hat{\mathbf{y}}_i}(z_i)} dz \tag{17}$$

where, $KL$ is the calculation formula of divergence, $\hat{\mathbf{y}} = [\hat{\mathbf{y}}_1, \hat{\mathbf{y}}_2, \cdots, \hat{\mathbf{y}}_N]$ is the estimated source signal vector after denoising, $\hat{\mathbf{y}}_i = [\hat{y}_i^1, \hat{y}_i^2, \cdots \hat{y}_i^F]$ represents the ith estimated source signal vector, $p_{\hat{\mathbf{y}}}(z)$ is the probability density of random variable $\hat{\mathbf{y}}$.

According to the scattering principle, the cost function of IVA could be expressed as

$$\begin{aligned} \mathcal{I}_{\text{IVA}} &\triangleq I[\hat{\mathbf{y}}_1, \cdots, \hat{\mathbf{y}}_N] \\ &= \sum_{n=1}^{N} H[\hat{\mathbf{y}}_n] - H(\hat{\mathbf{y}}_1, \cdots, \hat{\mathbf{y}}_N) \\ &= \sum_{n=1}^{N} H[\hat{\mathbf{y}}_n] - H\left(\mathbf{w}^{[1]}\hat{\mathbf{x}}^{[1]}, \cdots, \mathbf{w}^{[F]}\hat{\mathbf{x}}^{[F]}\right) \\ &= \sum_{n=1}^{N} H[\hat{\mathbf{y}}_n] - \sum_{k=1}^{F} \log\left|\det\left(\mathbf{w}^{[f]}\right)\right| - C. \end{aligned} \tag{18}$$

where, $H(\hat{\mathbf{y}}_n)$ represents the differential entropy of the $n$th source estimated component vector. According to linear transformation entropy $H(\hat{\mathbf{y}}) = \log|\det(\mathbf{w})| + H(\hat{\mathbf{x}})$, then $C = H(\hat{\mathbf{x}}^{[1]}, \cdots, \hat{\mathbf{x}}^{[F]})$ is a constant.

In the light of relation

$$H(\hat{\mathbf{y}}_n) = \sum_f H\left(\hat{y}_n^{[f]}\right) - I(\hat{\mathbf{y}}_n). \tag{19}$$

transform (20) into the following form

$$\mathcal{I}_{\text{IVA}} = \sum_{n=1}^{N}\left(\sum_{k=1}^{F} H\left(\hat{y}_n^{[f]}\right) - I\left(\hat{\mathbf{y}}_n\right)\right) - \sum_{k=1}^{F}\log\left|\det\left(\mathbf{w}^{[f]}\right)\right| - C. \quad (20)$$

It is known from (22) that the minimizing cost function minimizes the entropy of all components simultaneously and maximizes the mutual information within each estimated source component vector simultaneously. The mutual information calculation part of the cost function is the key to solve the "alignment" problem of multiple datasets.

The update matrix $\mathbf{w}$ is normalized, that is, the unit orthogonal matrix, which satisfies $\sum_{k=1}^{F}\log\left|\det\left(\mathbf{w}^{[f]}\right)\right| = 0$, so the cost function is simplified to

$$\mathcal{I}_{\text{IVA}} = \sum_{n=1}^{N}\left(\sum_{k=1}^{F} H\left(\hat{y}_n^{[f]}\right) - I\left(\hat{\mathbf{y}}_n\right)\right) - C. \quad (21)$$

#### 2) OPTIMIZATION METHOD

In order to derive an effective IVA separation algorithm, two methods, natural gradient and fast fixed point, are often used for optimization. However, the natural gradient method has a slow convergence speed and needs to choose an appropriate learning rate when optimizing the objective function.Here, the IVA algorithm based on fast fixed point (FastIVA) is adopted. The update of the demixing matrix of FastIVA algorithm does not need to select the iteration step size, and it has faster convergence speed. The iteration formula is

$$\mathcal{I}_{\text{IVA}} = \sum_{n=1}^{N} E\left[G\left(\left|\hat{\mathbf{y}}_n\right|^2\right)\right]. \quad (22)$$

where $G(z) = \sqrt{z}$ is a nonlinear function, $z$ is a dummy variable. Newton method is adopted to work out the extreme value of $\left[G\left(\left|\hat{\mathbf{y}}_n\right|^2\right)\right]$ under constraint $\hat{y}_n^f = \left(\mathbf{w}_n^f\right)^H \mathbf{x}^f$ and $\left\|\mathbf{w}_n^f\right\| = 1$, and the updated formula of the separation matrix obtained is

$$\mathbf{w}_n^{[f]} \leftarrow E\left[G'\left(\left|\hat{y}_n\right|^2\right) + \left|w_n^{[f]}\right|^2 G''\left(\left|\hat{\mathbf{y}}_n\right|^2\right)\right]\mathbf{w}_n^{[f]} - E\left[\left(\hat{y}_n^{[f]}\right)^* G'\left(\left|\hat{y}_n\right|^2\right)\hat{\mathbf{x}}^f\right]. \quad (23)$$

where, $\mathbf{w}_n^{[f]}$ is the $n$th row of update matrix $\mathbf{w}^{[f]}$, $G'(u) = dG(u)/du$ and $G''(u) = d^2G(u)/du^2$, $u$ is a dummy variable. After obtaining the updated matrix $\mathbf{w}^{[f]}$, it is standardized to ensure its orthogonality, and the standardization formula is as follows:

$$\mathbf{w}^{[f]} \leftarrow \left(\mathbf{w}^{[f]}\left(\mathbf{w}^{[f]}\right)^H\right)^{-1/2}\mathbf{w}^{[f]}. \quad (24)$$

where, $(\cdot)^H$ is conjugate transpose.

The denoise-FastIVA algorithm is shown below.

step 1: Input $\mathbf{x}_i(t)$.
step 2: Wavelet threshold denoising for $\mathbf{x}_i(t)$, output $\hat{\mathbf{x}}_i(t)$.
step 3: STFT $\hat{\mathbf{x}}_i(t)$, output $\hat{\mathbf{x}}_i(\omega)$.
step 4: Calculating initial separation matrix $\mathbf{w}^f$ using joint appro-
ximate diagonalization of eigen-matrices (JADE) algorithm
according [19].
step 5: Calculate estimated source $\hat{y}_n^{[f]}$.
step 6: $\mathbf{w}^{[f]} \leftarrow \left(\mathbf{w}^{[f]}\left(\mathbf{w}^{[f]}\right)^H\right)^{-1/2}\mathbf{w}^{[f]}$.
step 7: If the separation matrix is optimal, skip to the next step, other-
wise skip to step 5.
step 8: $\hat{\mathbf{y}}^f = \mathbf{w}^f\hat{\mathbf{x}}^f$.
step 9: ISTFT $\hat{\mathbf{y}}(\omega)$, output $\hat{\mathbf{s}}(t)$.

## IV. SIMULATION EXPERIMENTS AND DISCUSSIONS

In this section, the simulated communication convolution mixed signal is used for separation, and the Pearson correlation coefficient and bit error rate (BER) are used as the performance evaluation indicators of signal separation.

### A. SEPARATION PERFORMANCE

About separation results of convolution mixed signals with noise, this paper uses correlation coefficient and BER to evaluate the performance of the separation algorithm.

#### 1) CORRELATION COEFFICIENT

The correlation coefficient can be used to reflect the linear correlation degree between two random variables. Assuming there are two variables, $X$ and $Y$, the correlation coefficients between the two variables can be calculated as follows

$$\rho_{X,Y} = \frac{\text{cov}(X,Y)}{\sigma_X\sigma_Y} = \frac{E\left((X-\mu_X)(Y-\mu_Y)\right)}{\sigma_X\sigma_Y} = \frac{E(XY)-E(X)E(Y)}{\sqrt{E\left(X^2\right)-E^2(X)}\sqrt{E\left(Y^2\right)-E^2(Y)}} \quad (25)$$

where $cov(X,Y)$ is covariance of $X$ and $Y$. $\sigma_X$ and $\sigma_Y$ are the standard deviations of $X$ and $Y$, respectively. $\mu_X$ and $\mu_Y$ are the mean values of $X$ and $Y$, respectively. $E(\cdot)$ means the mean.

#### 2) BIT ERROR RATE

BER is a measure of the accuracy of data transmission over a specified time.

$$BER = \frac{\text{Number of error bits in transmission}}{\text{Total number of bits transmitted}} \times 100\% \quad (26)$$

where, $\times$ is multiplication operation.

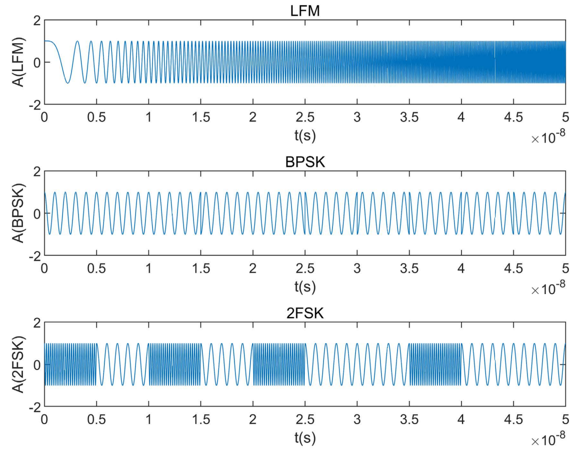


(a) Source signal waveform

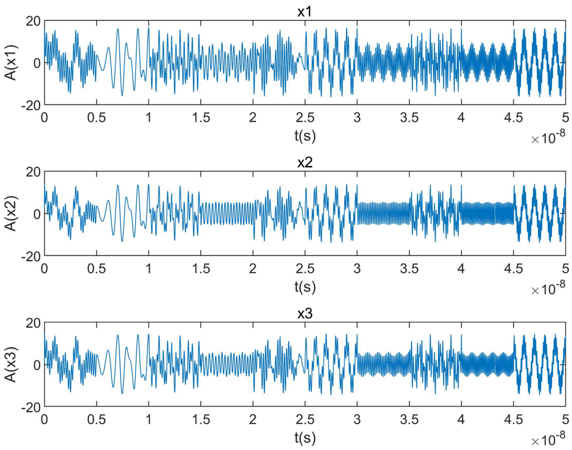


(b) Noisy observation signal

**FIGURE 3.** **Waveform diagram of source signal and observation signal. The baseband signals of BPSK and 2FSK are {1110010101} and {1010100100} respectively. The task of blind separation is to separate the source signal from the observed signal.**

### *B. SIMULATION RESULTS*

This section realizes the separation of three independent modulation signals through simulation experiments. In the simulation, three kinds of modulation signals with 50000 sample points are generated by MATLAB. The first signal is a linear frequency modulation (LFM) signal with a center frequency of 5GHz; The second signal is a BPSK signal with a carrier of 100MHz, resulting in a total of 10 code element; The third signal is a 2FSK signal with carrier divided into 100MHz and 500MHz, resulting in a total of 10 code element. The waveform is shown in Fig.3 (a). In subsequent experiments, $A(\cdot)$ is used to indicate the amplitude. Three modulation signals are passed through a 10-order convolution filter, and the filter coefficients follow a Gaussian distribution in the range [0, 1]. The mixed signals are obtained by adding g aussian white noise with SNR of 30dB. Waveforms are as shown in Fig.3 (b):

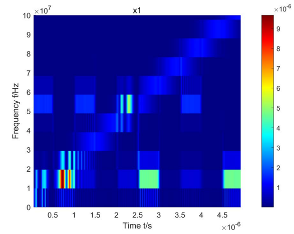


(a)

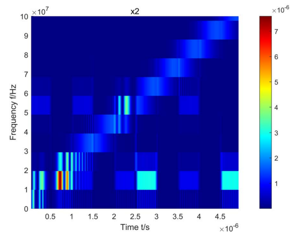


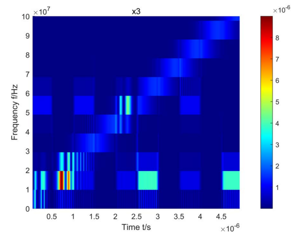


(b) (c)

**FIGURE 4.** **Observation signal STFT time-frequency diagram.**

**TABLE 1.** **Correlation coefficient between source signal and separation signal with noise.**

| $\rho$ | FDICA | FastIVA |
|---|---|---|
| LFM | 0.8648 | 0.8815 |
| BPSK | 0.7555 | 0.8387 |
| 2FSK | 0.7528 | 0.8143 |

#### 1) NOISY SIGNAL SEPARATION SIMULATION

After the observation signals are obtained, the observation signals need to be whitened processing firstly. Then the observed signal is transformed into the frequency domain by STFT. Hanning window is selected as the window function of STFT, with the length of 1024 and the sliding length of 768. Its time-frequency diagram is shown in Fig.4 (a), (b) and (c):

FDICA method is used to separate the frequency domain mixed signal obtained by STFT. The FastIVA method used in this paper uses JADE algorithm to get initial values, and Newton method for optimization, so the FastIVA method used in this paper is more complex. However, FDICA has random uncertainty in sorting the results at each frequency point. This experiment takes advantage of greater correlation between homologous adjacent frequency points to sort each frequency point, and the results are as follows Fig.5 (a). In addition, the frequency domain mixed signals are separated using the FastIVA algorithm. The separation results are shown in Fig.5 (b). From the waveform of the recovery signal, FastIVA separates better overall, and FDICA distorts part of the separated 2FSK signal. FastIVA can basically recover three modulated signals. Table 1 is given by calculating the correlation coefficient between the source signal and the separated signal.

FDICA only has a good separation effect on LFM signals, and the correlation coefficient is 86.48%. It has a poor separation effect on 2FSK signals and BPSK signals. The correlation coefficients of the three modulation signal separation

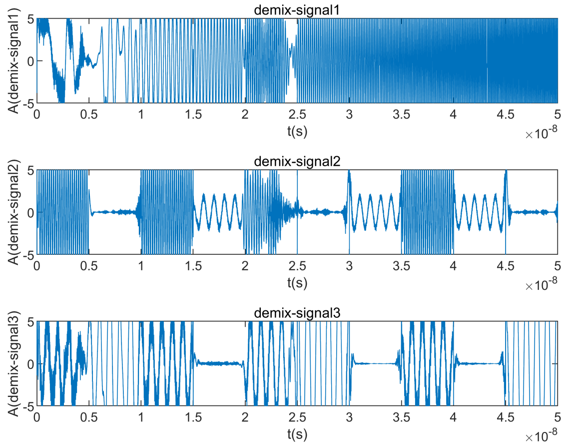


(a) Separation results of FDICA

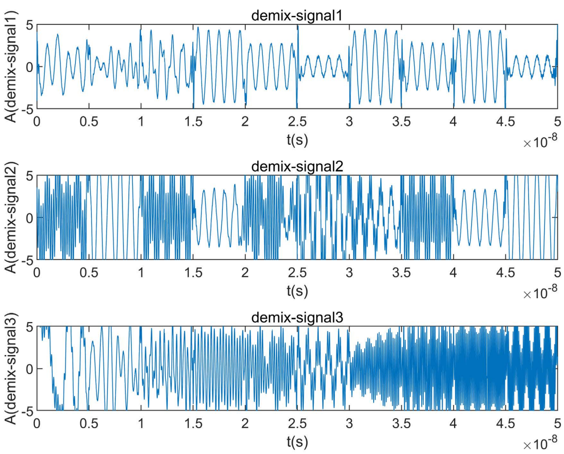


(b) Separation results of FastIVA

**FIGURE 5. Separation results of noisy mixed signals.**

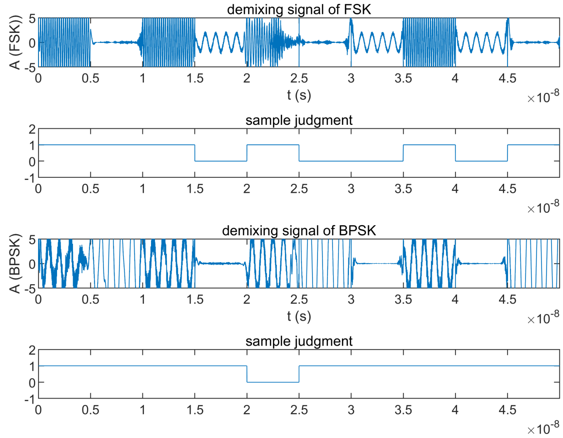


(a) FDICA

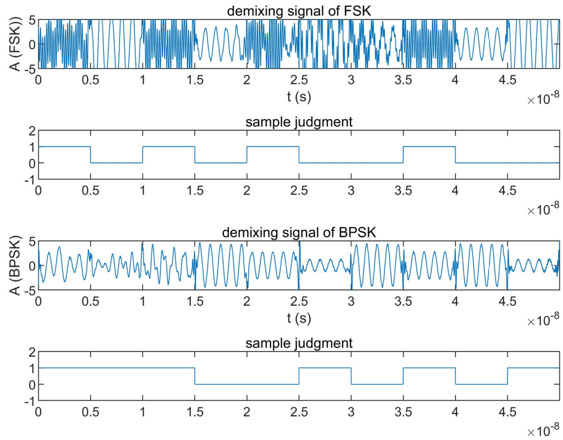


(b) FastIVA

**FIGURE 6. Demodulation result of noisy separated signal.**

obtained by FastIVA method are 81% and above, which can separate convolution mixed signals well. Combined with the separated waveform graph, FastIVA is better than FDICA in separating convoluted mixed signals of three modulated signals.

The separated BPSK and 2FSK signals are demodulated and the waveforms are obtained as shown in Fig. 6 (a) and (b). When demodulating separated 2FSK and BPSK signals, SER of FDICA separated 2FSK signals is 20%, and BER of BPSK signals is 30%. FastIVA separated 2BSK and BFSK signals demodulate the baseband signal completely and correctly without error codes.

### 2) DENOISING SIGNAL SEPARATION SIMULATION

The 30dB white Gaussian noise is considered in the convolution mixed signal. Formula (5) shows that noise has some influence on signal separation. After receiving the noisy observation signal, wavelet threshold denoising is performed on the noisy mixed signal, and then FDICA is used to separate the mixed signal. The algorithm is defined as denoise-FDICA. The result waveforms of denoise-FDICA and denoise-FastIVA separation are shown in Fig. 7 (a) and Fig. 7 (b), respectively. Analyzing the waveforms in Figure 7(a) and (b), the separation effect of denoise-FastIVA is better. Compared to Fig. 5(b), the waveform of Fig. 7(b) is more similar to the source signal waveform.

Calculate the correlation coefficient of each separated signal and the source signal to get Table 2.

**TABLE 2. Correlation coefficient between source signal and de-noise separate signal separated signal.**

| $\rho$ | denoise-FDICA | FastIVA | denoise-FastIVA |
|---|---|---|---|
| LFM | 0.8801 | 0.8815 | 0.9473 |
| BPSK | 0.7831 | 0.8387 | 0.9758 |
| 2FSK | 0.7569 | 0.8143 | 0.9553 |

After denoising the observed signal, the correlation coefficient calculated by signal separation can be significantly improved. Compared with the similarity of FastIVA demixed results, the correlation coefficient of LEM signal

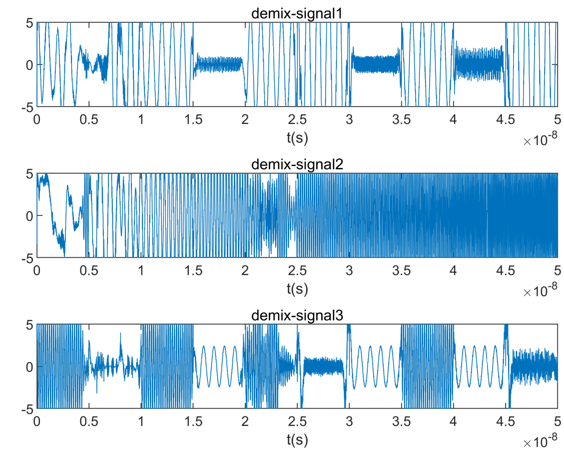


(a) denoise-FDICA

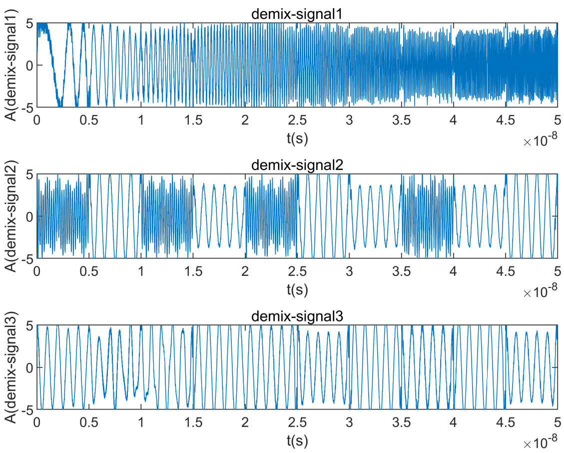


(b) denoise-FastIVA

**FIGURE 7.** **Denoising mixed signal separation saveform.**

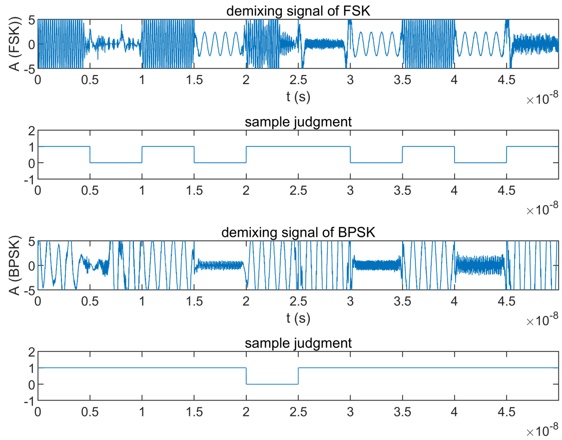


(a) denoise-FDICA

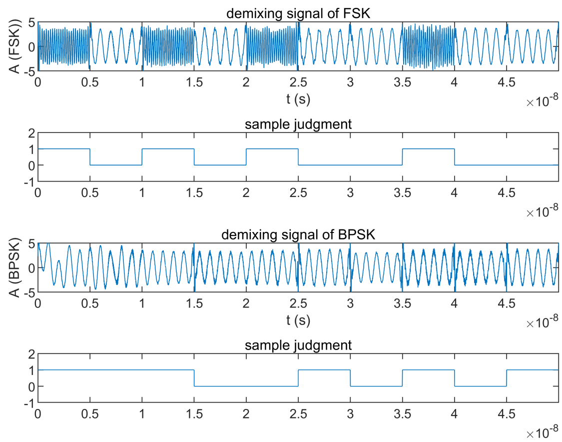


(b) denoise-FastIVA

**FIGURE 8.** **Demodulation results of denoising mixed signal separation results.**

increased from 88.15% to more than 94.73%. The correlation coefficient of BPSK signal enhanced from 83.87% to more than 97.58%. the correlation coefficient of 2FSK signal improved from 81.43% to over 95.53%.

The correlation coefficient between the signal and the source signal separated utilizing the denoise-FastIVA method is more than 94%. It shows that the separated signal has a strong correlation with the source signal, and the denoise-FastIVA can well separate the convolution mixed signal with noise.

Demodulate the BPSK and 2FSK signals in the separated signals obtained making use of denoise-FDICA and denoise-FastIVA. The baseband signals gained are shown in Fig. 8 (a) and (b).

In Fig. 8, the result of 2FSK signal demodulation obtained by denoise-FDICA does not appear error codes, which is lower than that of the demodulation of separated signal of FDICA. The denoise-FastIVA separates the demodulated baseband signal without error codes. Experiments show that under the condition of SNR=30dB, compared with the traditional algorithm, denoise-FastIVA has a certain improvement in the separation effect of convolution mixed signals.

### *C. SEPARATION SIMULATION UNDER DIFFERENT SIGNAL-TO-NOISE RATIO CONDITIONS*

Noise has some influence on the algorithm. In previous experiments, only 30dB noise signal is considered. Demixing of separation algorithms considering different SNR. The correlation coefficient between the separated signal and the source signal is calculated as shown in Fig. 9.

As can be seen from Fig. 9, when $0\text{ dB} < \text{SNR} < 30\text{ dB}$, compared with the traditional separation algorithm, the denoise-FastIVA proposed in this paper can better separate the source signal. Under the condition of $0\text{ dB} < \text{SNR} < 5\text{ dB}$, the correlation coefficient of the denoise- Fastiva separated signal is $60\% \sim 80\%$, and the source signal can be basically recovered. Under the condition of $5\text{ dB} < \text{SNR} <$

**TABLE 3. Separate signal demodulation results.**

| SNR | signal | denoise-FDICA | BER | FastIVA | BER | denoise-FastIVA | BER |
|---|---|---|---|---|---|---|---|
| 0dB | BPSK | 1100000111 | 30% | 1111010101 | 10% | 1110010101 | 0 |
| 0dB | 2FSK | 1110111100 | 30% | 1011000101 | 30% | 0000100000 | 30% |
| 5dB | BPSK | 1010111101 | 30% | 1111010101 | 10% | 1110010101 | 0 |
| 5dB | 2FSK | 1011111110 | 30% | 0011101100 | 30% | 1010100110 | 10% |
| 10dB | BPSK | 1010000100 | 30% | 1110010101 | 0 | 1110010101 | 0 |
| 10dB | 2FSK | 1011000100 | 20% | 1011101110 | 30% | 1010100100 | 0 |
| 20dB | BPSK | 1111011111 | 30% | 1110010101 | 0 | 1110010101 | 0 |
| 20dB | 2FSK | 1010110101 | 20% | 1010100100 | 0 | 1010100100 | 0 |
| 30dB | BPSK | 1111011111 | 30% | 1110010101 | 0 | 1110010101 | 0 |
| 30dB | 2FSK | 1110100101 | 20% | 1010100100 | 0 | 1010100100 | 0 |

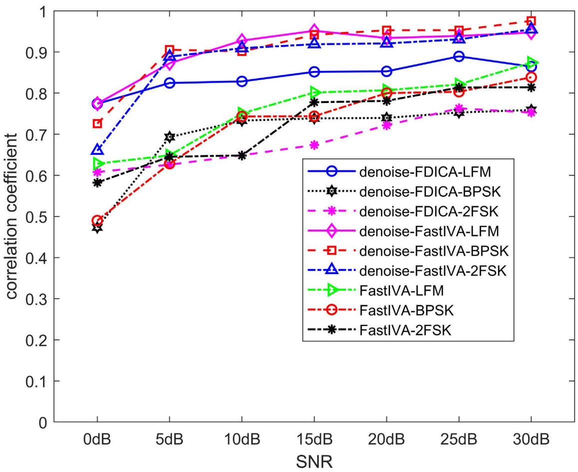


**FIGURE 9. Separation correlation coefficients at different SNR.**

10 dB, the correlation coefficient of denoise-Fastiva method separated signal is above 80%, which can separate mixed signals well. When 10 dB $<$ SNR $<$ 30 dB, the correlation coefficient of the denoise-FastIVA separated signal can reach more than 90%, and the mixed signal can be very well separated.

Demodulate BPSK and 2FSK in the separated signal and calculate the BER. The results are shown in Table 3.

Table 3 shows that BPSK and 2FSK signals separated by denoise-FDICA and FastIVA methods have error bits when demodulated under 0 dB $<$ SNR $<$ 10 dB conditions. The demodulation result of denoise-FastIVA only has 2FSK signal demodulation errors occur. There is no error symbol in the demodulation of demixing result of the denoise-FastIVA when 10 dB $<$ SNR $<$ 30 dB, but denoise-FDICA separation results showed wrong symbols in demodulation. When 10 dB $<$ SNR $<$ 20 dB, FastIVA demixing result demodulates with error symbols.

To further analyze the separation of denoise-FastIVA methods, the simulation model shown in Fig. 10 is designed for analysis.

One signal sends 100 bits baseband signal, and after 2FSK modulation, the carrier frequencies are 100MHz and 500MHz, respectively. One signal sends 100 bits

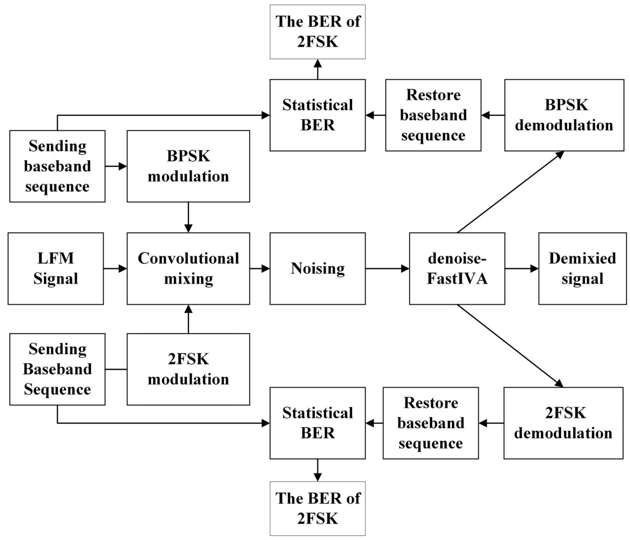


**FIGURE 10. System simulation model.**

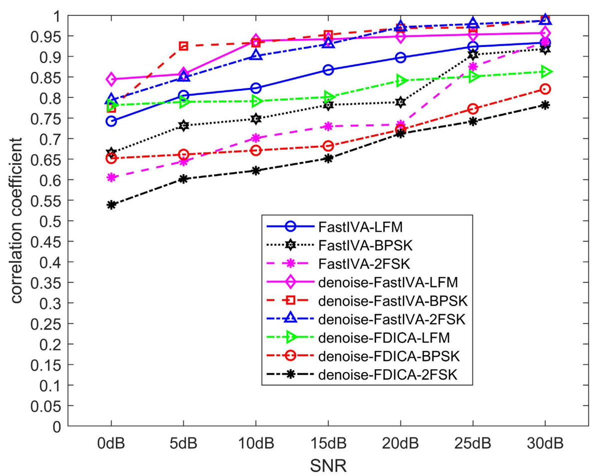


**FIGURE 11. Separation correlation coefficients at different SNR.**

baseband signal, passes BPSK modulation, carrier frequency is 500MHz. The two signals are then convoluted and mixed with LFM signal with a center frequency of 5GHz. After adding some noise, it is separated by denoise-FastIVA algorithm to demodulate BPSK and 2FSK signals in the separated signal, and the BER is calculated.

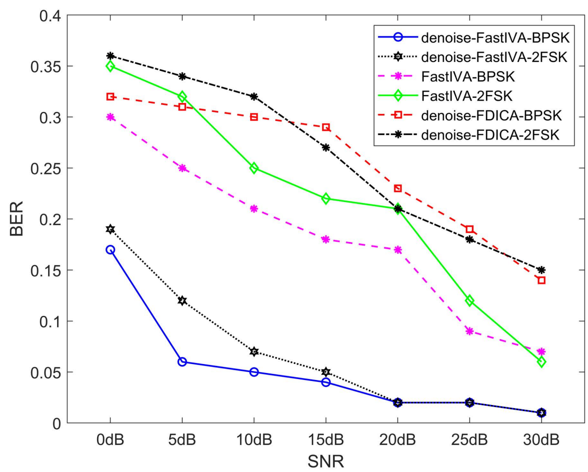


**FIGURE 12.** **BER for separate signal demodulation.**

Each signal contains 50000 sample points, Separating mixed signals using different separation algorithms. In this section, each separation algorithm is tested 20 times under the same conditions, and the optimal results are obtained. the mixed signal is separated by a separation algorithm as shown in Fig.11 and Fig.12.

Figure 11 shows the curve of the correlation coefficient of the separated signal with the SNR under different SNR conditions. It can be seen that the performance of the three separation methods decreases with the decrease of SNR. When $0\,\text{dB} < \text{SNR} < 30\,\text{dB}$, compared with the two other separation methods, the denoise-FastIVA proposed in this paper can better separate the source signal. When $5\,\text{dB} < \text{SNR} < 30\,\text{dB}$, the denoise-FastIVA method has the best separation effect. Under condition $10\,\text{dB} < \text{SNR} < 30\,\text{dB}$, The correlation coefficients of signals separated by denoise-FastIVA method can both be more than 90%, and the signal can be better separated.

Fig.12 shows the BER curves of BPSK and 2FSK separated by different separation methods with different SNR. It can be seen that with the decrease of SNR, the performance of the three separation methods decreases. When $0\,\text{dB} < \text{SNR} < 30\,\text{dB}$, compared with the two other separation methods, The BER of BPSK signal and The BER of 2FSK signals in the demixing signal obtained by the denoise-FastIVA are lower. The denoise-FastIVA has the best separation performance. When $20\,\text{dB} < \text{SNR} < 30\,\text{dB}$, both BER of BPSK and BER of 2FSK signals are 2%, denoise-FastIVA can separate signals very well. Under condition $10\,\text{dB} < \text{SNR} < 20\,\text{dB}$, the BER of BPSK and 2FSK increased gradually, but both were less than 7%, denoise-FastIVA can separate signals well. When $0\,\text{dB} < \text{SNR} < 5\,\text{dB}$, The BER of 2FSK signal is more than 10%, and the denoise-FastIVA method is poor.

## V. CONCLUSION

In the wireless communication system, noise has a great influence on frequency domain blind source separation algorithm, so the research on noise reduction and separation is of great significance. In this paper, a denoising IVA convolution mixed frequency domain blind signal separation algorithm is studied. The principle is to denoise the noisy observation signal using the wavelet threshold denoising method to reduce the influence of noise on the IVA algorithm. The algorithm separates three modulation signals under different SNR, which makes the IVA algorithm have better anti-noise ability.

How to separate convolution mixed signals under low signal-to-noise ratio and strong interference conditions is an important research direction in the future. And this paper only considers the wavelet threshold denoising method. Other denoising methods will be studied in the future.

## REFERENCES

[1] Z. Luo, C. Li, and L. Zhu, "A comprehensive survey on blind source separation for wireless adaptive processing: Principles, perspectives, challenges and new research directions," *IEEE Access*, vol. 6, pp. 66685–66708, 2018.

[2] H. Sawada, N. Ono, H. Kameoka, D. Kitamura, and H. Saruwatari, "A review of blind source separation methods: Two converging routes to ILRMA originating from ICA and NMF," *APSIPA Trans. Signal Inf. Process.*, vol. 8, no. 1, 2019.

[3] H. M. Salman, "Speech signals separation using optimized independent component analysis and mutual information," *Science*, vol. 2, no. 1, pp. 1–6, 2021.

[4] A. Hyvärinen and E. Oja, "Independent component analysis: Algorithms and applications," *Neural Netw.*, vol. 13, nos. 4–5, pp. 411–430, Jun. 2000.

[5] S. Hu, Y. Hu, X. Wu, J. Li, Z. Xi, and J. Zhao, "Research of signal denoising technique based on wavelet," *TELKOMNIKA Indonesian J. Electr. Eng.*, vol. 11, no. 9, pp. 5141–5149, Sep. 2013.

[6] R.-M. Zhao and H.-M. Cui, "Improved threshold denoising method based on wavelet transform," in *Proc. 7th Int. Conf. Model., Identificat. Control (ICMIC)*, Dec. 2015, pp. 1–4.

[7] X. Liu, H. Wang, and Y. Huang, "SCBSS signal de-noising method of integrating EEMD and ESMD for dynamic deflection of bridges using GBSAR," *IEEE J. Sel. Topics Appl. Earth Observ. Remote Sens.*, vol. 14, pp. 2845–2856, 2021.

[8] R. Zhou, J. Han, T. Li, and Z. Guo, "Fast independent component analysis denoising for magnetotelluric data based on a correlation coefficient and fast iterative shrinkage threshold algorithm," *IEEE Trans. Geosci. Remote Sens.*, vol. 60, pp. 1–15, 2022.

[9] R. Prasad, H. Saruwatari, and K. Shikano, "Enhancement of speech signals separated from their convolutive mixture by FDICA algorithm," *Digit. Signal Process.*, vol. 19, no. 1, pp. 127–133, Jan. 2009.

[10] S. M. M. Islam, O. Boric-Lubecke, and V. M. Lubekce, "Concurrent respiration monitoring of multiple subjects by phase-comparison monopulse radar using independent component analysis (ICA) with JADE algorithm and direction of arrival (DOA)," *IEEE Access*, vol. 8, pp. 73558–73569, 2020.

[11] P. Lin, Z. Wang, and Y. Chen, "A blind source separation sorting algorithm for sonar echo signal based on frequency-point amplitude correlation," in *Proc. IEEE Int. Conf. Electr. Eng., Big Data Algorithms (EEBDA)*, Feb. 2022, pp. 905–909.

[12] Z. Luo, R. Guo, and C. Li, "Independent vector analysis for blind deconvolving of digital modulated communication signals," *Electronics*, vol. 11, no. 9, p. 1460, May 2022.

[13] H. Sawada, R. Mukai, S. Araki, and S. Makino, "A robust and precise method for solving the permutation problem of frequency-domain blind source separation," *IEEE Trans. Speech Audio Process.*, vol. 12, no. 5, pp. 530–538, Sep. 2004.

[14] V. G. Reju, S. N. Koh, and I. Y. Soon, "A robust correlation method for solving permutation problem in frequency domain blind source separation of speech signals," in *Proc. IEEE Asia Pacific Conf. Circuits Syst. (APCCAS)*, Dec. 2006, pp. 1891–1894.

[15] T. Kim, I. Lee, and T.-W. Lee, "Independent vector analysis: Definition and algorithms," in *Proc. Fortieth Asilomar Conf. Signals, Syst. Comput.*, 2006, pp. 1393–1396.

[16] S. Erateb, M. Naqvi, and J. Chambers, "Online IVA with adaptive learning for speech separation using various source priors," in *Proc. Sensor Signal Process. Defence Conf. (SSPD)*, Dec. 2017, pp. 1–5.
[17] Q. Long, S. Bhinge, V. D. Calhoun, and T. Adali, "Independent vector analysis for common subspace analysis: Application to multi-subject fMRI data yields meaningful subgroups of schizophrenia," *NeuroImage*, vol. 216, Aug. 2020, Art. no. 116872.
[18] H. Zhang and W. Wei, "Convolutive frequency-domain blind interference-signal separation algorithm based on IVA," *J. Mil. Commun. Technol.*, vol. 33, no. 3, p. 6, 2012.
[19] S. M. M. Islam, E. Yavari, A. Rahman, V. M. Lubecke, and O. Boric-Lubecke, "Separation of respiratory signatures for multiple subjects using independent component analysis with the JADE algorithm," in *Proc. 40th Annu. Int. Conf. IEEE Eng. Med. Biol. Soc. (EMBC)*, Jul. 2018, pp. 1234–1237.

**MINGCHUN LI** received the B.S. degree in communication engineering from the Sichuan University of Science and Engineering (SUSE), Zigong, China, in 2020. She is currently pursuing the master's degree with the Sichuan University of Science and Engineering, Yibin. Her research interest includes blind source separation.

**ZHENGWEI CHANG** received the Ph.D. degree in computer application technology from the University of Electronic Science and Technology of China (UESTC), in 2009. Since 2009, he has been with the State Grid Electric Power Research Institute, where he is currently a Professor, since January 2019. His research interests include artificial intelligence, smart grid, and the Internet of Energy.

**LINGHAO ZHANG** received the Ph.D. degree in computer software and theory from Nanjing University, in 2014. He is currently a Senior Engineer of the Energy Internet Technology Center, State Grid Sichuan Electric Power Research Institute. His research interests include electric power big data analysis, artificial intelligence, and cyber-physical systems. In recent years, he has won many awards in cyber security and big data competitions, as a principal investigator or major research participant, he has worked on more than ten science and technology projects from U.S. National Science Foundation, China 863, State Grid Corporation, and Sichuan Provincial Government et al.

**HOUDONG XU** received the M.S. degree in power system and automation from Tsinghua University, in 2005. He is currently the Deputy Director with the Department of Digitalization, State Grid Sichuan Electric Power Company. His research interests include big data analysis, 5G communication, and green low-carbon technology.

**ZHONGQIANG LUO** (Member, IEEE) received the B.S. and M.S. degrees in communication engineering and pattern recognition and intelligent systems from the Sichuan University of Science and Engineering, Zigong, China, in 2009 and 2012, respectively, and the Ph.D. degree in communication and information systems from the University of Electronic Science and Technology of China (UESTC), in 2016. Since 2017, he has been with the Sichuan University of Science and Engineering, where he is currently an Associate Professor. From December 2018 to December 2019, he was a Visiting Scholar with the Department of Computer Science and Electrical Engineering, University of Maryland, Baltimore County (UMBC). His research interests include information fusion, blind source separation, signal processing for wireless communication systems, and intelligent signal processing.

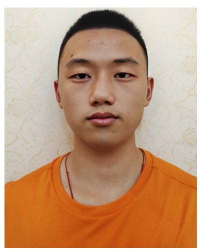

**RUIMING GUO** received the B.S. degree in communication engineering and its automation from the Chengdu College of University of Electronic Science and Technology, Chengdu, China, in 2021. He is currently pursuing the M.S. degree with the Sichuan University of Science and Engineering. His main research interest includes blind source separation.